Modelling time dependent flow fields over three dimensional dunes

R.J. Hardy, T.I. Marjoribanks
Department of Geography, Durham University, UK

D.R. Parsons, A.J. Reesink, B. Murphy
Geography, Environment and Earth Sciences, University of Hull, UK

P.J. Ashworth
Geography and Environment, University of Brighton, UK

J.L. Best
Departments of Geology, Geography and Geographic Information Science, University of Illinois at Urbana-Champaign, USA.

ABSTRACT: The flow field over dunes has been extensively measured in laboratory conditions and there is now a general understanding of the nature of the flow over dunes formed under equilibrium flow conditions. However, fluvial systems typically experience unsteady flow and therefore the sediment-water interface is constantly responding and reorganizing to this unsteadiness, over a range of both spatial and temporal scales. This is primarily through adjustment of bed forms (including ripples, dunes and bar-forms) which then subsequently alter the flow field. This paper investigates, through the application of a Large Eddy Simulation (LES) model, the influence of these roughness elements on the overall flow and the variation in flow resistance during a change in flow conditions. To provide boundary conditions and a validation dataset for the LES model, a series of physical experiments were undertaken in a flume, 16m long and 2m wide, where fine sand (D_{50} of 239µm) was water worked under a range of unsteady hydraulic conditions that generated a series of quasi-equilibrium three-dimensional bed forms. During the experiments flow was measured with a series of acoustic Doppler velocimeters. On four occasions, the flume was drained and the bed topography measured with terrestrial LiDAR to create digital elevation models. LES was used to simulate the three-dimensional time-dependent flow fields over the four static bed topographies from the experiments. The numerically predicted flows were analyzed by standard Reynolds decomposition approaches and a Lagrangian coherent flow structure identification method. The results show that superimposed bed forms, that are common to bed form fields adjusting to changes in flow conditions, can cause changes in the nature of the classical separated flow regions in the lee side of dunes. In particular, the number of locations where vortices are shed and the points of flow reattachment, which effect the time dependent prediction of shear stress, were found to alter substantially. This has significant implications for sediment entrainment and sediment transport dynamics and the results enable improved process understanding of three dimensional nature of bed form adjustment to changes in flow conditions.

1 INTRODUCTION

Bed forms in river channels perpetually adjust to non-uniform and unsteady flow conditions, with marked changes in flow causing hysteresis-effects in bed roughness, sediment transport rates and morphodynamics. Dunes are a common fluvial bed form feature, forming in a range of sediment sizes from silt and sand through to gravel (Dinehart, 1992; Best, 1996; Carling, 1999; Kleinhans, 2001; Kleinhans 2002; Carling *et al*., 2005). Their presence significantly influences the mean and turbulent flow which subsequently exerts a strong control on the entrainment, transport and deposition of sediment (Parsons *et al.,* 2005, Best, 2005). In recent years there has been an increased understanding of dune dynamics due to significant advances in monitoring flow and dune morphology both in the laboratory and field (Best, 2005). This research has determined that the main flow characteristics associated with dunes dynamics are; i) accelerating flow over the dune stoss side; ii) flow separation or deceleration (Nelson *et al*., 1993; McLean *et al*., 1994; Best & Kostachuck, 2002) from the dune crest in the lee side; iii) flow reattachment at 4-6 dune heights downstream (Engel, 1981); iv) a shear layer between the separated flow and stream wise flow above which it expands as it extends downstream and; v) an internal boundary layer that grows from the reattachment point along the stoss slope of the next dune downstream. However, virtually all process understanding has been deduced from work that has dealt with morphologies that are essentially regular and two-dimensional; a situation that is rare in natural river channels. Moreover, bed form adjustment to non-uniform and unsteady flow conditions, that is known to cause hysteresis-effects in bed roughness, has largely been ignored in terms of the flow fields

and morphological response. Of the recent work that does exist, Kleinhans (2004) indicated that the reduction in dune size through cannibalization by smaller superimposed dunes differs fundamentally from bedform amalgamation during dune growth (Coleman and Melville 1994; Raudkivi & Witte, 1990). These adjustments in bed form morphology (whether ripples, dunes and bar-forms), during changes in flow conditions, alter the channel and bed roughness and therefore have a large effect on the overall flow field. Here we analyze the influence of three-dimensional dunes on the flow field through the application of a Large Eddy Simulation (LES) model where boundary conditions and validation are taken from physical scale experiments.

2 METHODOLOGY

2.1 *Numerical Solution*

The numerical scheme solves the full three-dimensional Navier-Stokes equations discretised using a finite-volume method. The interpolation scheme used is hybrid-upwind, where upwind differences are used in high convection areas (Peclet number > 2) and central differences are used where diffusion dominates (Peclet number < 2). The pressure and momentum equations are coupled by applying SIMPLEST, a variation on the SIMPLE algorithm of Patankar and Spalding (1972). Convergence can precede either smoothly or with damped oscillations to the final solution. To achieve relaxation either: (i) realistic maximum and minimum values may be imposed on the solution; or (ii) relaxation may be used to limit the amount of change allowed in any variable at a given iteration. Weak linear relaxation was used for the pressure correction, while weak false time step relaxation was used for the other variables. The convergence criterion was set such that the residuals of mass and momentum flux were reduced to 0.1% of the inlet flux. The initial simulations use a Re-normalized Group theory (RNG) κ-ε turbulence models. These results are then used as initial conditions for the LES simulations where a standard Smagorinsky (1963) sub-grid model was applied. The LES simulations were run at a frequency of 10Hz for 102.4 seconds.

The upstream inlet boundary conditions is specified from experimental data (see below) and the downstream outlet is specified as a fully developed flow profile with the hydrostatic pressure set at the surface at the downstream outlet. The dune topography is from the experimental data (see below, Fig. 1). The topography was then subsequently included into the discretisation using a mass flux scaling approach. The approach uses a regular structured grid in which all control volumes are orthogonal in both computational and Cartesian space, and the bed topography specified using cell porosities where the cell volume and faces are scaled and blocked according to the amount of topography included in the mesh. This approach has been developed (Lane *et al.,* 2003; Hardy *et al.,* 2005) and applied from millimeter scales of gravel beds (Lane *et al.,* 2004; Hardy *et al.,* 2007) through to river reaches of approximately 1 km (Hardy *et al.,* 2006; Sandbach *et al.,* 2012). For topography at a scale smaller than that of the computational discretization, the non-equilibrium form of the standard wall functions is used (Launder & Spalding, 1974). This form of the equations assumes a local equilibrium of turbulence and is suitable at boundary cells that contain both bed and water and is also suitable in cells with separation. The roughness height is parameterized as half the spatial discretization, however, CFD schemes are typically not sensitive to roughness parameterizations (Lane, 2005). Applying this method provides an approach to understand the way in which complex dune morphology interacts with the associated three dimensional flow field. The second advantage of this scheme is that it maintains a constant filter length throughout the domain and allows LES numerically stable simulations to be undertaken.

2.2 *Experimental Design: Laboratory*

A recirculating flume 16m long (*l*), 2m wide (*w*) and 0.5m deep (*h*) was constructed in the Total Environment Simulator in The Deep at the University of Hull, UK. The flume contained a sand bed with a D_{50} of 239μm. The experimental runs covered a range of transient conditions, where the magnitudes and rates of change in discharge (and hence flow velocity) and depth were carefully controlled and systematically increased and decreased. Water-depth and water surface slope along the flume were measured, at 2 Hz, using 7 water elevation probes. Flow velocity was measured at 25 Hz with 4 aDv's set at 40% of the water depth at 4 locations in the test section to provide an approximation of average flow velocity. The hydraulic conditions used are reported in Table 1.

Table 1: The hydraulic conditions used as boundary conditions in the numerical simulations that replicate those in the flume experiments

	Inlet Velocity at 0.4 z/h (ms^{-1})	Avg Water depth (m)	Froude Number (-)	Reynolds Number $\times 10^3$ (-)
Exp. 1	0.49	0.151	0.36	127
Exp. 2	0.53	0.165	0.36	157
Exp. 3	0.74	0.184	0.56	218
Exp. 4	0.51	0.136	0.35	134

Bed elevation was measured over a 5 m test section at repeat intervals of 7.5 and 300 seconds. These elevations were mapped throughout the 120 hours of

experiments using a multi-frequency (1, 2 and 4 MHz) acoustic backscatter profiler that measured bed elevation together with acoustic backscatter (for later determination of suspended sediment concentration from sample calibrations). Vertical resolution of the bed elevation measurements was 2.5 mm and horizontal resolution was 5 mm. On 4 separate occasions the flume was slowly drained and the full three dimensional topography was measured at higher resolutions and broader extents with a terrestrial laser scanner, which provided the necessary topographic boundary conditions (Fig. 1).

2.3 *Model Geometry and Boundary conditions.*

For the purpose of the numerical experiments, a 3m long (*l*) and 1m wide (*w*) section of dunes was used to define the bed geometry. The computational domain was regular in the *x, y, z* directions, with a grid resolution of 0.005m. In the *z* direction, to allow inclusion of topography data using the mass flux scaling treatment, the maximum extent of the domain was set depending on the height of the dunes plus the water depth and ranged from 0.235 to 0.325 m depending on the scale of the dunes. Thus, the computational grid was sized at 600 (*nx*) × 200 (*ny*) × (47-58 *nz*) (5 640 000 to 7 800 000 grid cells). The topography (Fig. 1) demonstrates a range of dune topographies for which to test the model.

Visual analysis of all four DEM's clearly demonstrates the three dimensional nature of the topography. Primarily, in none of the experiments are the dune ridges parallel to the side walls nor are they continuous across the width of the domain. This is in direct contrast to several previous experiments discussed previously which consider regular and two-dimensional dunes. Experiment 1 appears to contain the greatest range of topographic scales with larger dunes present with smaller scale topography (ripples) superimposed. Similar observations can be made for both Experiment 2 and 4 although there are slightly more regular structures. The topography formed in experiment 3, formed under the highest hydraulic conditions, shows a form closer to a smooth bed with only two very shallow dunes formed.

2.4 *Model Validation*

In order to validate the model time averaged aDv measurements are compared to the Reynolds averaged model results. This is only for four points in the domain and is acknowledged that this is not ideal, however, due to the scaling relationships used in the experimental design of the flume experiments the subsequent water depths (Table 1) were shallow. With the unconsolidated sand bed (D_{50} of 239µm) and the presence of an aDv in the flow, caused shear and scouring of the bed thus modifying the topography. Model validation used an automated correspondence algorithm to match aDv measurement locations to corresponding grid cell locations. The size of the model grid cells was 0.005 m while the aDv measures in a 0.08 m diameter cylindrical sampling volume, with a height of 0.01 m. Thus, it determines a spatially-averaged velocity that corresponds approximately to 25 grid cells.

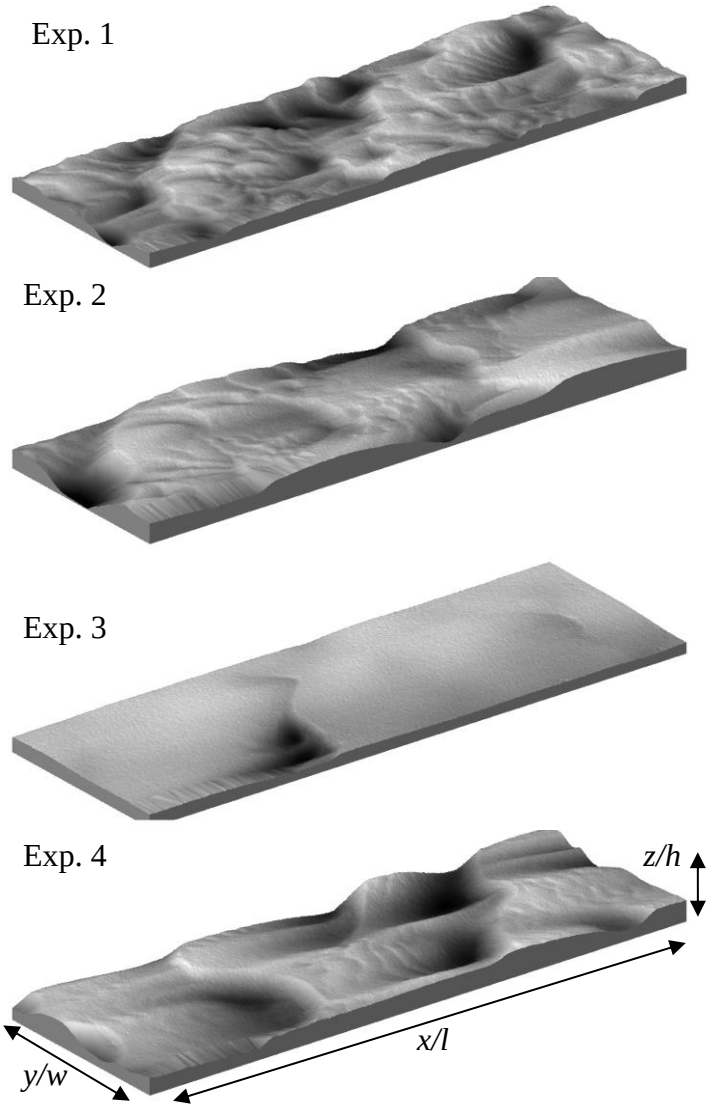

Figure 1: The Digital Elevation Models measured using Terrestrial LIDAR used in the numerical experiments. The hydraulic conditions at the end of the physical experiments before the experiments were stopped, the flume drained and measured using a terrestrial laser scanner are reported in table 1.

In the presence of strong shear in the flow, this opens up the possibility of high velocity variability in model predictions that will not be captured in the ADV measurements. Thus, the average, standard deviation and range of model predictions corresponding to each aDv measurement location were determined. In general, the model and the aDv measurement were with 5% for the mean flow conditions. Furthermore, previous examples of applying this modelling scheme have shown good agreement (Hardy *et al.*, 2012) with reported squared correlation coefficients (r^2) between the aDv measurements

and the CFD model for the downstream (*u*-) component including 0.89 (Ferguson *et al.,* 2004), 0.95 (Bradbrook *et al.,* 1998) and 0.91 (Lane *et al.,* 2004) for a range of environmental applications. These applications demonstrate the strong predictive ability of the numerical scheme and that it can therefore be used with confidence in the numerical experiment we report herein.

2.5 *Modelled Flow Analysis*

Initially, the spatial prediction of flow is analyzed through the velocity magnitude. This is calculated by resolving the downstream (*u*-), cross-stream (*v*-) and vertical (*w*-) component of velocity. This provides a means of analyzing general flow characteristics but not localized flow direction.

The analysis is then extended to vortex detection methods in order to link the individually identified flow structures to the overall pattern of flow. Typically, Eulerian vortex methods have been applied to an instantaneous velocity field by analyzing spatial patterns in the velocity gradient field and its invariants (Green *et al.,* 2007). The bases of most identification methods is the Q criterion (Hunt *et al.,* 1988), where Q is the second invariant of divergence of the velocity vector and implies that a vortex is present if the magnitude of the vorticity is greater than the strain. This criterion has subsequently been developed to include the λ criterion (Jeong & Hussain, 1995), Δ criterion (Chong *et al.,* 1990) and the swirl strength criterion (Zhou *et al.,* 1999). In all of these approaches turbulent structures are defined only as areas where the criterion is greater than a predefined threshold. When there is a time dependent velocity field, as used in this application with the LES data, Lagrangian vortex methods can be used to identify the temporal convergence (or divergence) of flow into vortices. These methods apply a similar theory to those described above, whereby individual particles within the fluid are tracked through time, and their progressive separation calculated. The changes in relative distance between neighboring trajectories through time is quantified using Lyapunov exponents and have also been shown to be a useful tool in identifying vortices within flows (Haller, 2000; Haller & Yuan, 2000; Haller, 2005). Specifically Lyapunov exponents measure the degree to which the phase space is stretched through time and as such are an extension of eigenvalues in that they describe the magnitude of distortion with respect to the principal directions and are therefore analogous to eigenvectors. Whereas eigenvalues are local, Lyapunov exponents are considered global as they are averaged to obtain the infinite-time behavior of the entire system. They are more commonly referred to as finite-time Lyapunov exponents (FTLE) which can be used to project trajectories either forwards or backwards in time. If particle trajectories are projected backwards the FTLE highlights regions of the flow which act as attractors within the flow (Haller & Yuan, 2000). Similarly, if projected forward, the FTLE to identifies repelling regions in the flow (Green *et al.,* 2007) with regions of high FTLE identifying vortices, also known as Lagrangian coherent structures (LCS) (Haller, 2000; Haller & Yuan, 2000). In particular, ridges within the FTLE field correspond to coherent flow structures (Shadden *et al.,* 2005), and therefore in order to identify vortices within the flow, it is necessary to study the derivative of the FTLE field to identify local maxima, rather than simply find the globally extreme values.

3 RESULTS

3.1 *Three dimensional flow*

The results are presented here focus primarily on the flow over Experiment 1 and 3 DEM's as these have the greatest differences in their three dimensional topographies. The numerical predictions for Experiment 1 are shown in Figure 2.

The figure shows the periodic nature of the flow. In general the classical flow model associated with dunes of acceleration of stream wise flow along the stoss side of the dune, flow separation and reattachment several dune heights downstream is not observed. However, regions of faster flow, forming shear may be identified in all simulations (Fig. 2, i) down the midline of the domain. Below this a separated lower velocity flow zone just behind the dune crests can be observed. In addition, parcels of higher velocity fluid can be traced across the dunes and interact with the bed forms, therefore increasing the magnitude of the flow (Fig. 2, line ii). None of these high velocity flow structures appear to extend across the entire width of the domain and their greatest spatial width is less than 0.5 *y/w*. Reattachment is not observed and appears spatially less extensive than that observed with straight-crested dunes. It is suggested that this is associated with the several scales of complex three dimensional topography.

When the range of topography is reduced (Experiment 3, Fig. 3) similar patterns are observed. There is a region of high magnitude flow forming a shear layer that extends through the entire domain (middle *y/w* slice) and below this region and area or separated flow. In addition, the parcels of higher momentum flow are observed moving through the domain although their lateral extent appears smaller than those for the rougher bed.

Again classical flow separation and reattachment is not observed in the simulations. This may be associated with using the velocity magnitude and a flow descriptor (a scalar value) and looking at single velocity components (*w*-, vertical component) may prove more beneficial. However, it is clear to see

that the three dimensional dune morphology is heavily influencing the flow structures.

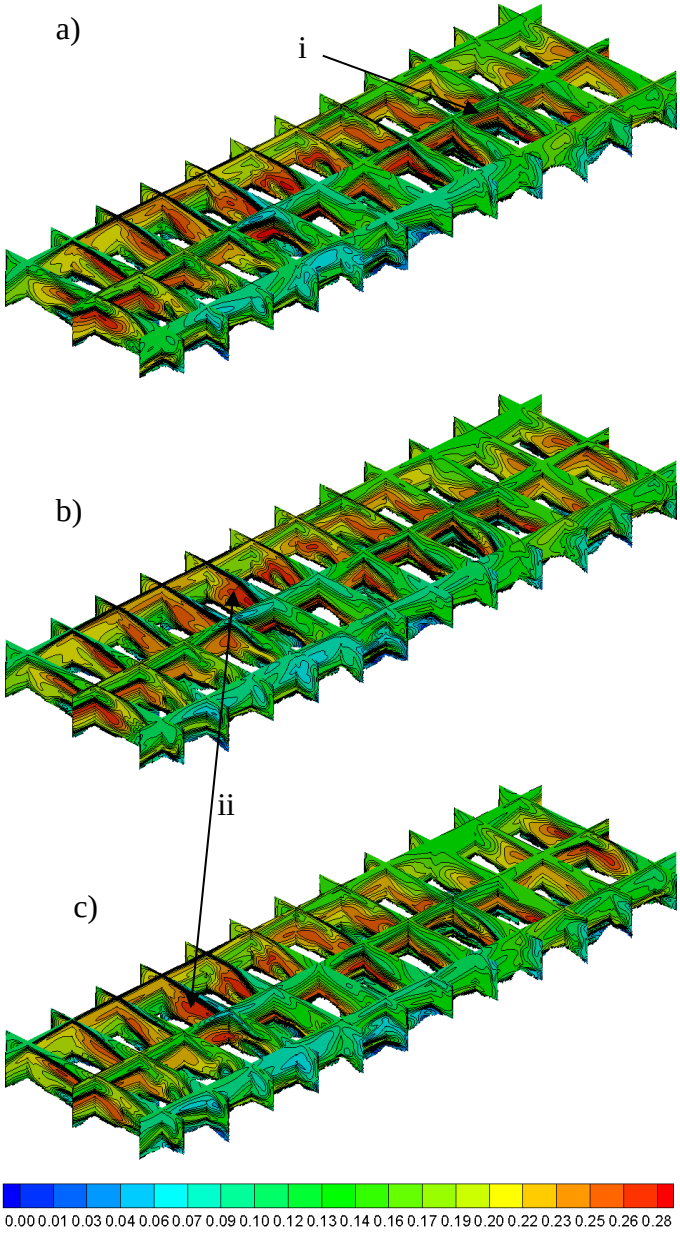

Figure 2: Three dimensional velocity magnitude for Experiment 1 for three separate time periods; a= *t*, b) *t*+60 seconds & c) *t*+120seconds. The dune topography has been blanked. In all images flow is from left to right. The white region represents topography that is blocked out of the domain using the MFSA.

3.2 *Flow structure identification*

In order to further assess the flow structures, to try to determine the origin and explore their temporal coherence, FTLE was calculated for both experiment 1 and 3. The technique requires a temporal starting point, so the result half way through simulation was chosen for this initial analysis. Secondly, the length of time that the structures are tracked back need to be prescribed. In this application a sensitivity test was undertaken and structures were tracked back for 0.5, 1, 2 and 5 seconds to assess how long the Lagrangian Coherent flow structures existed and the distance that they had travelled. Full three-dimensional FTLE was calculated but the results are presented as two dimensional (*x*-*y* planes) for predetermined heights (*z*/*h*). The results for Experiment 1 are presented in Figure 4.

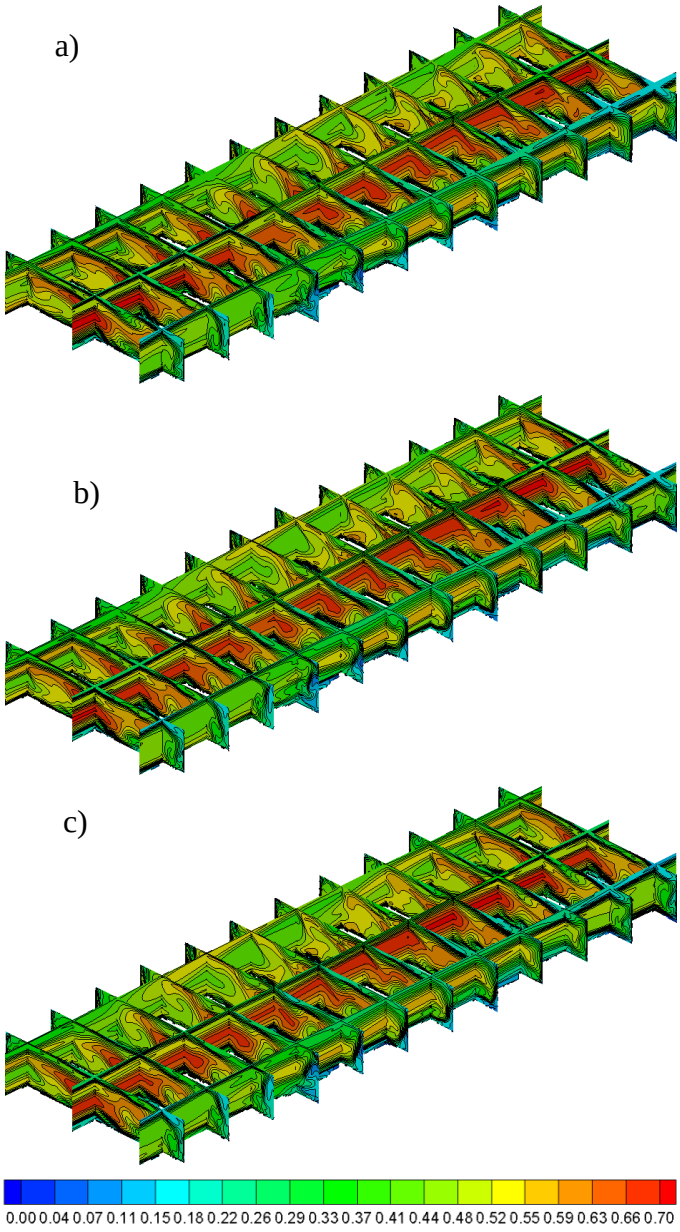

Figure 3: Three dimensional velocity magnitude for Experiment 3 for three separate time periods; a= *t*, b) *t*+60 seconds & c) *t*+120seconds. In all images flow is from left to right. The white region represents topography that is blocked out of the domain using the MFSA.

In Figure 4a the flow is tracked back for 1 second at a flow height of 0.32 *z*/*h* where the crest of some of the dunes can be observed in the flow field. Packets of high FTLE are observed behind each dune crest (Figure 4a, region i) with ridges of high FTLE moving between crest to crest. It is suggested that these regions are formed in flow reattachment regions and the turbulence then follows predefined flow paths determined by the topography. These crests represent Lagrangian Coherent flow structures and there appears to be a distinct linkage between

the dunes. These flow paths are still detectable in the flow field higher above the dune crests (Figure 4b, *z/h* 0.4) although the widths of the linkages have narrowed and are more defined. These flow structures appear to be orientated with the dune crest (approximately at 30° to the side walls) with some quite significant steering of flow paths (Fig. 4b, ii). These become far more significant and cover a greater spatial area when then structures are tracked back for 5 seconds (Fig. 4c). They are located in the reattachment region behind the crests, which suggest that multiple scales of structure are originating from these regions. Although not investigated here, these are potential sediment transport paths due to the increase turbulent kinetic energy and Reynolds stresses within the dune field.

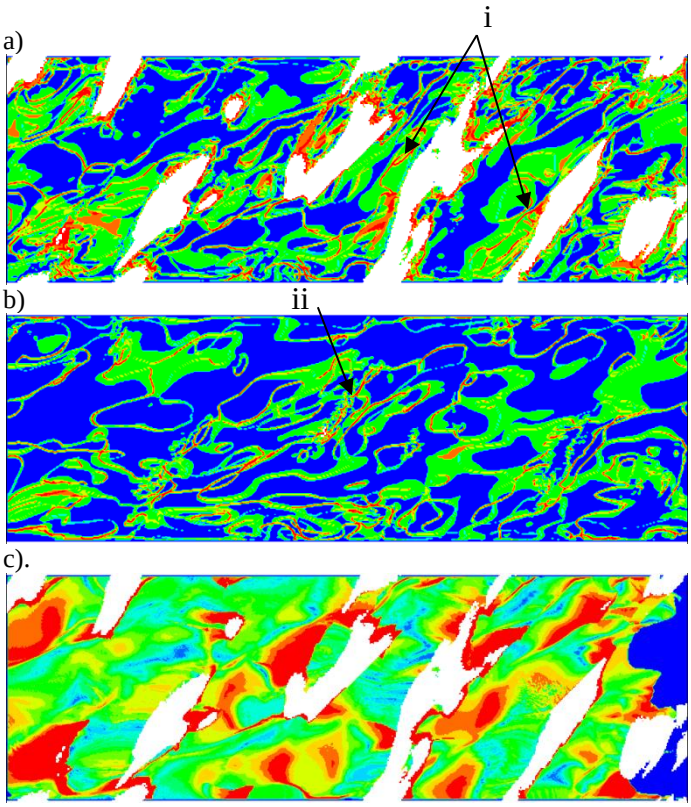

Figure 4: FTLE for Experiment 1 for a) 0.32 *z/h* tracking back 1 seconds; b) 0.3 *z/h* tracking back 1 seconds and; c) 0.32 *z/h* tracking back 5 seconds. In all images flow is from left to right. The white region represents topography that is blocked out of the domain using the MFSA. The closer to the red color the stronger the attraction of flow.

The same analysis technique is applied to Experiment 3 (Fig. 5). In this example the topographic protrusion is far less but again high regions of FTLE are detected behind the dune crest with linkages of turbulent flow structures again following predefined topographic paths between crests (Fig. 5a, line i). A similar trend, to the one observed in experiment 1, is observed higher in the flow (Fig. 5b & c) with the flow structure paths becoming narrower but still orientated at the same angle to the dune crest throughout the flow depth.

The examples demonstrated here have tracked back over a range of spatial resolutions but have always started at the same time within the numerical simulation. It is therefore necessary to extend this analysis to consider different starting times to assess whether these structures demonstrate spatial coherence and consistently follow the same topographically steered path through time.

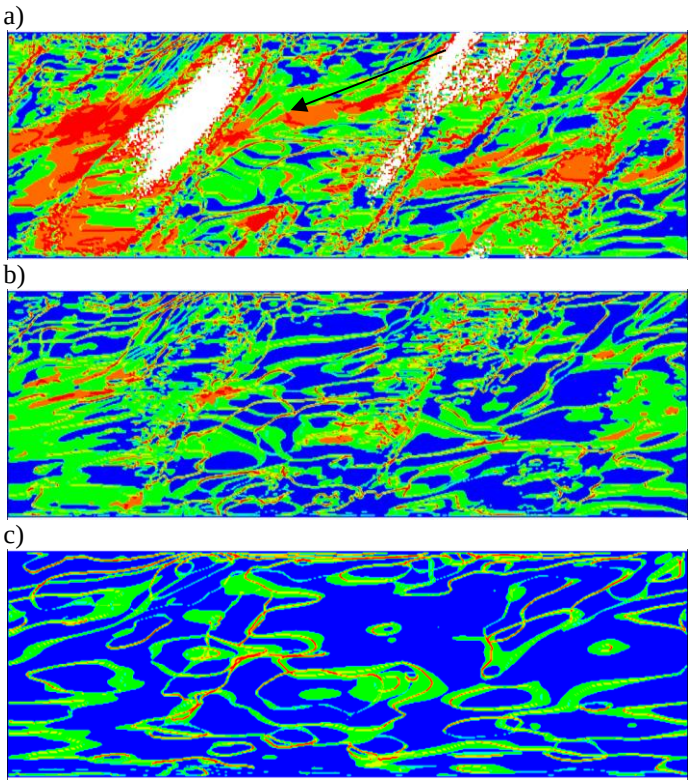

Figure 5: FTLE for Experiment 3 for a) 0.3 *z/h* tracking back 1 seconds; b) 0.4 *z/h* tracking back 1 seconds and; c) 0.5 *z/h* tracking back 1 seconds.

4 CONCLUSIONS

The three-dimensionality in dune morphology has been shown to significantly influence the flow structure across a range of bed conditions. These results of the time-dependent flow fields have several important implications for dune dynamics that encompass sediment entrainment, deposition, sediment transport rates, dune migration and thus the overall stability of a sand bed river (Parsons *et al.*, 2006). The classical flow model derived from studying two dimensional dunes does not appear valid for these examples. Previous work has shown that the smaller separation zones and lower velocity gradients associated with the leeside of three dimensional dunes may be associated with a smaller level of large-scale turbulence intensities (Maddux *et al.*, 2003). This would imply that the spatially-averaged bed shear stress is likely to be less which would have implications for the amount of sediment entrained into suspension (e.g. Jackson 1976, Kostaschuk & Church 1993). However, the vortex detection methods applied here have shown that there are common flow

path linkages between the dunes, steered by the topography, where turbulence is high. These are potentially important in determining the sediment transport paths through the dune field due to the localized increase in turbulent kinetic energy and Reynolds stresses.

ACKNOWLEDGEMENTS

This research was funded on NERC Grant NE/I01456X/1. Data presented in this paper can be obtained from contacting RJH.

REFERENCES

Best, J.L. 1996. The fluid dynamics of small-scale alluvial bedforms, in P. A. Carling & M. R. Dawson (eds), *Advances in Fluvial Dynamics and Stratigraphy*: 67–125, John Wiley, Hoboken, N. J.

Best, J.L. 2005. The fluid dynamics of river dunes: A review and some future research directions. *Journal of Geophysical Research* 110: F04S02.

Best, J.L., & R.A. Kostaschuk 2002. An experimental study of turbulent flow over a low-angle dune, *Journal of Geophysical Research*, 107(C9): 3135,

Bradbrook, K.F., Biron, P., Lane, S.N., Richards, K.S. & Roy, A.G. 1998. Investigation of controls on Secondary circulation and mixing processes in a simple confluence geometry using a three-dimensional numerical model *Hydrological Processes* 12: 1371-1396.

Carling, P.A. 1999. Subaqueous gravel dunes, *Journal of Sedimentary. Research* 69: 534–545.

Carling, P.A., Richardson, K. && Ikeda, H. 2005. A flume experiment on the development of subaqueous fine-gravel dunes from a lower-stage plane bed *Journal of Geophysical Research* 110: F04S05.

Chong, M.S.,Perry, A.E. & &Cantwell, B.J. 1990. A general classification of three-dimensional flow fields *Physics of Fluids A: Fluid Dynamics* 2(5): 765-777.

Coleman, S.E. & Melville B.W., 1994, Bedform development. *Journal of Hydraulic Engineering* 120: 544-560.

Dinehart, R.L. 1992. Evolution of coarse gravel bedforms – Field measurements at flood stage *Water Resources Research* 28(10): 2667–2689.

Engel, P., & Lau Y.L. 1980. Computation of bed load using bathymetric data *Journal of Hydraulic Division, . Am. Soc. Civ. Eng.* 106: 380– 639.

Ferguson, R.I., Parsons, D.R. Lane, S.N. & Hardy, R.J. 2003. Flow in meander bends with recirculation at the inner bank *Water Resources Research* 39(11): 1322.

Green M.A., Rowley C.W. & Haller G. 2006. Detection of Lagrangian coherent structures in three-dimensional turbulence *Journal of Fluid Mechanics* 572: 111–120.

Haller, G. 2001: Distinguished material surfaces and coherent structures in 3D fluid flows *Physica D* 149: 248–277.

Haller, G 2005: An objective definition of a vortex *Journal of Fluid Mechanics* 525: 1-26.

Haller, G. & G. Yuan (2000). Lagrangian coherent structures and mixing in two-dimensional turbulence. *Physica D: Nonlinear Phenomena* 147(3–4): 352-370.

Hardy, RJ, Lane, SN, Lawless, Best. JL MR. Elliot, L. & Ingham, DB. 2005). Development and testing of numerical code for treatment of complex river channel topography in three-dimensional CFD models with structured grids. *Journal of Hydraulic Research*, 43(5): 468-480.

Hardy, RJ, Parsons, DR, Best, JL, Lane SN, Kostaschuk, R. & Orfeo, O. 2006. Three-dimensional numerical modelling of flows over a natural dune field. In: *River Flow 2006*, Ferreria, RML, Alves ECTL, Leal JGAB & Cardos, AH. (Eds). Taylor & Francis Group, London. p. 1077-1083. ISBN 0-415-40815-6.

Hardy, R. J., S. N. Lane, R. I. Ferguson, & D. R. Parsons 2007, Emergence of coherent flow structures over a gravel surface: A numerical experiment, *Water Resources Research* 43: W03422.

Hardy, R.J., Lane, S.N. & Yu, D. 2011. Flow structures and mixing at an idealized bifurcation: a numerical experiment *Earth Surface Processes & Landforms* 36(15): 2083-2096.

Hunt, J.C.R., Wray, A.A. & Moin, P. 1988. Eddies, stream, and convergence zones in turbulent flows, Center for Turbulence Research Rep. CTR-S88.

Jackson, R.G. 1976. Sedimentological and fluid-dynamic implications of turbulent bursting phenomena in geophysical flows, *Journal of Fluid Mechanics* 77: 531-560.

Jeong, J. & F. Hussain 1995. On the identification of a vortex. *Journal of Fluid Mechanics* 285: 69-94.

Kleinhans, M.G. 2001. The key role of fluvial dunes in transport and deposition of sand-gravel mixtures, a preliminary note, *Sedimentary Geology* 143: 7 –13.

Kleinhans, M.G. 2002. PhD thesis at the University of Utrecht, The Netherlands, NGS 293.

Kleinhans, M.G. 2004. Sorting in grain flows at the lee side of dunes *Earth-Science Reviews* 65(1): 75-102.

Kostaschuk R.A. & Church M. A. 1993. Macroturbulance generated by dunes: Fraser River, Canada, *Sedimentary Geology* 85*:* 25-37.

Lane, SN, Hardy, R.J. Elliot, L., & Ingham, D.B. 2003. High resolution numerical modelling of three dimensional flows over complex river bed topography, *Hydrological Processes* 16: 2261-2272.

Lane, S.N. 2005. Roughness - time for a re-evaluation? *Earth Surface Processes and Landforms* 30(2): 251-253.

Lane, S.N., Hardy, R.J. Elliott, L. & Ingham, D.B. 2004. Numerical modeling of flow processes over gravelly surfaces using structured grids and a numerical porosity treatment, *Water Resources Research* 40(1): 18.

Launder, B.E. & Spalding, D.B., 1974. The numerical computation of turbulent flows. *Computer Methods in Applied Mechanics and Engineering* 3: 269-89.

Maddux, T.B., Nelson, J.M. & McLean, S.R. 2003. Turbulent flow over three-dimensional dunes: 1. Free surface and flow response *Journal of Geophysical Research, Earth-Surface* 108(F1): F16009.

Mclean, S.R., Nelson, J. & Wolfe, S.R. 1994. Turbulence structure over two-dimensional bedforms: Implications for sediment transport. *Journal of Geophysical Research* 99: 729-12,747.

Nelson, J., Mclean, S.R., Wolfe, S.R. 1993. Mean Flow and Turbulence Fields over Two Dimensional Bedforms. *Water Resources Research* 29: 3935-3953.

Patankar, S.V. & Spalding D.B., 1972. A calculation procedure for heat, mass and momentum transport in three-dimensional parabolic flows *International Journal of Heat and Mass Transfer* 15: 1782.

Parsons, D.R., Best, J.L., Orfeo, O., Hardy, R.J., Kostaschuk, R. & Lane, S.N., 2005, Morphology and flow fields of three-dimensional dunes, Rio Parana, Argentina: Results from simultaneous multibeam echo sounding and acoustic Doppler current profiling. *Journal of Geophysical Research-Earth Surface*, 110:

Parsons, DR, Best, JL, Lane, SN, Hardy, RJ, Kostaschuk, R, Shugar, D & Orfeo, O. 2006. Morphology, flow and sediment transport over a natural 3D dune field: Rio Paraná, Argentina. IAHR *River Flow 2006*, Third International Conference on Fluvial Hydraulics, Lisbon, Portugal.

Raudkivi, A.J. & Witte, H-H., 1990. Development of bed features. *Journal of Hydraulic Engineering* 116: 1063-1079.

Sandbach, SD, S.N. Lane, R.J. Hardy, M.L. Amsler, P.J. Ashworth, J.L. Best, A.P. Nicholas, O. Orfeo, D.R. Parsons, A.J.H. Reesink, G.H. Sambrook-Smith & R.N. Szupiany (2012) Roughness length representation in 3D numerical simulations of large rivers *Water Resources Research:*

Shadden, S. C., F. Lekien & J. E. Marsden (2005). Definition and properties of Lagrangian coherent structures from finite-time Lyapunov exponents in two-dimensional aperiodic flows. *Physica D-Nonlinear Phenomena* 212(3-4): 271-304.

Smagorinsky, J. (1963). General Circulation Experiments with primitive equation, *Monthly Weather Review* 91(3): 99-164.

Sprott, J. C. 2003. *Chaos and Time Series Analysis*. Oxford, Oxford University Press.

Zhou, J., Adrian R.J., Balachandar, S. & Kendall, T. M. 1999. Mechanisms for generating coherent packets of hairpin vortices in channel flow. *Journal of Fluid Mechanics* 387: 353-396.